THE PUBLISHING HOUSE
OF THE ROMANIAN ACADEMY

PROCEEDINGS OF THE ROMANIAN ACADEMY, Series A,
Volume 22, Number 4/2021, pp. 343–351

MACROSCOPIC MECHANICAL PROPERTIES AND MECHANISM OF SUPERFINE PORTLAND CEMENT-BASED COMPOSITE SEALING MATERIAL FOR GAS DRAINAGE

Sheng XUE[1], Xin GUO[1], Chunshan ZHENG[1], Yaobin LI[1], Linfang Xie[2]

[1] Anhui University of Science & Technology, School of Safety Science and Engineering, Huainan, China
[2] Henan Provincial Communications Planning & Design Institute Co Ltd, Zhengzhou, Henan, China
Corresponding author: Xin Guo, E-mail: guoxin190510@163.com

Abstract. Superfine Portland cement is a kind of inorganic grouting material widely used, which can be used to prepare cementitious material with short solidification time, high strength and good effect on micro-crack grouting, which is of great significance to the prevention and control of coal mine gas disaster. This paper combines macroscopic mechanical property test and microstructure observation to study the mechanical properties and mechanism, the hydration products, and microstructure of superfine cement-based composite sealing materials. The results show excessive additives will lead to defects and decrease the mechanical properties of the composite material. The results of SEM and XRD analysis show that the hydration of superfine cement-based sealing materials produces a large amount of Aft (Calcium aluminate hydrated from cement hydration products combined with sulfate ions can make cement structure more compact). The more sufficient the hydration, the more compact the overall microstructure and the higher the mechanical property. The study also shows that the composite material containing 8% expansion agent, 0.3% water reducer and 0.03% retarder has high mechanical properties and low cost.

Key words: sealing material, superfine cement, microstructure, mechanical properties, expansion agent, water reducer, hydration products.

1. INTRODUCTION

China is the country with the most serious gas disaster accidents, and gas drainage is the most effective means to control gas disaster. When drilling is constructed, a large number of fractures will be generated around the borehole, and these fractures also provide a pathway for the diffusion of gas. In order to suppress the diffusion of gas and reduce the probability of coal mine gas disasters, it is necessary to use sealing materials to seal the cracks around the borehole. With the continuous development of China's coal resources, the mining depth increases at a rate of 10–25 m per year [1], Due to high temperature and high in-situ stress in the coal seam, and the mining stress, the drainage borehole is prone to deformation and collapse, which challenges gas drainage and threatens the safety of coal mine production. The sealing material is required to have a certain compressive strength [2–5].

The factors affecting the mechanical properties of sealing materials include the water-cement ratio [6–7], the use of early strength agents [8–9] and the composition of raw materials [10–14]. The currently used sealing materials include inorganic sealing materials, represented by cement mortar, gypsum, clay, etc. and organic sealing materials including Marisan, polyurethane, etc. Cement mortar, gypsum, clay, etc. is easy to shrink after curing and has poor injectability [15–16]. Marisan and polyurethane are expensive and have poor durability [17–18]. In recent years, to achieve zero discharge of underground waste, coal chips, gangue and other materials have been applied to the research and development of sealing materials. The composite grouting material prepared with binders and other materials has lower porosity, fewer holes, larger skeleton density, and higher compactness, and therefore higher macroscopic mechanical strength [19–21]. Glass fiber reinforced cement-based materials with high strength and excellent impermeability have been widely applied into the field of construction and environment [22–23]. The addition of polycarboxylate superplasticizer can

reduce the consistency of the material and improve the mechanical properties of the material on the basis of improving the fluidity of the material [24–26]. In addition, some studies have found that capillary crystalline materials [27], steel slag [28–29] and silica fume [30] can improve the mechanical properties of cement mortar, and are added to the sealing material as raw materials.

Scholars have found that superfine cement has higher strength, environmental friendliness, and good permeability and groutability similar to organic chemical sealing materials [31], but research in the field of sealing materials is rare. In this paper, the superfine cement-based composite sealing material is prepared by using superfine cement as the base material, and water reducing agent and other materials as additives that this material falls into the category of pastes. The hydration products were characterized with the XRD analysis method to study the mechanical properties of composite sealing material.

2. EXPERIMENTAL MATERIALS AND METHODS

2.1. Experimental materials

Superfine Portland cement, the gray powder prepared by vibration grinding of cement clinker mixed with 5 % $CaSO_4 \cdot 2H_2O$ from China Cement Plant, was combined with the HCSA expander, the gray-white powder, as shown in Table 1. The polycarboxylic acid water reducing agent (PCE) with the water reducing rate of 20–35% used in this research was a white powder, easily soluble in water. Seaweed powder, the white powder easily soluble in water was selected as the retarder. The solution of seaweed powder and water, which was colorless and transparent, was made with the mass ratio of 1:130, and then added to the cement base.

Table 1

Chemical composition of materials/%

Chemical composition	w (SiO_2)	w (Al_2O_3)	w (Fe_2O_3)	w (CaO)	w (MgO)	w (SO3)	Loss
HCSA expansion agent	1.50	15.61	1.37	50.60	2.08	27.50	1.19
Superfine Portland Cement	20.75	4.90	3.61	65.00	1.09	2.01	2.54

2.2. Experimental methods

To study the effect of admixture content on the mechanical properties of composite materials, five groups of composite materials with different admixture content were designed as shown in Table 2.

Table 2

Mix proportions of composite materials

NO	Water-cement ratio	Superfine cement content/g	Mixing ratio of each component/%		
			water reducing agent	retarder	expansion agent
A1	0.8:1	2000	0.5	0.04	9
A2	0.8:1	2000	0.5	0.05	10
A3	0.8:1	2000	0.4	0.04	8
A4	0.8:1	2000	0.3	0.03	8
A5	0.8:1	2000	0	0	0

The sample preparation process is: weighing the corresponding quality of water and cement. The amount of the corresponding dosage of the additive weighed by the electronic balance was slightly more than the actual amount. The cement is pre-stirred with appropriate amount of water, and then the admixture is fully dissolved with appropriate amount of water. The admixture is gradually mixed with cement according to the post-mixing method. In order to prevent air from entering the slurry and stirring unevenly and then affect the later compressive strength test data, the electric stirrer is usually used to stir 2–3 min twice at a low speed. In the stirring process, the speed should not be too fast and the speed should be kept uniform. The cement slurry was poured into the 70 mm × 70 mm × 70 mm triple mold, and the demoulding agent should be evenly smeared around the mold to prevent the demoulding failure or damage to the test block. The mold

was placed in a constant temperature and humidity cement curing box with the curing temperature and humidity of 20 °C and 97 %, respectively. The mold could be removed by a demoulding air gun after 12 h of curing. After removing the mold, the test block was placed in the same environment to continue to be cured to the corresponding age.

a) preparation of specimen

b) compressive strength tests

Fig. 1 – Preparation and compressive strength test of samples.

The uniaxial compressive strength of the composites was tested by the RMT pressure testing machine as shown in Fig. 1b. Displacement control was used. The loading speed was 0.001 mm/s until the specimen was damaged. The axial displacement was measured by the 50 mm displacement sensor and the axial load was measured by the 1000 kN force sensor.

The environmental electron scanning microscope FEI Quanta 200 FEG, with the operating acceleration voltage of 0.5～30 kV, magnification of 30～300,000 times, and the resolution of 3.0 nm was used to study the microstructure of the composite materials. The microscope mainly uses secondary electron signal imaging, which can produce an enlarged image to observe the surface morphology of the sample. This image was established in time sequence when the sample was scanned. The experimental operating system and principle are shown in Fig. 2.

Fig. 2 – Scanning electron microscope.

SmartLab X-ray diffractometer (Cu target, the voltage of 40 kV, current of 30 mA, speed of 8°/min, step size of 0.02°/step, scanning range of 5°~90°, normal test temperature) was used for XRD analysis. The powder samples were fixed with the positive pressure method, and the data were processed by MDI JADE 6.5 software. The test conditions of each group of samples were the same. The incident beam made each scatterer re-radiate a small part of the intensity as a spherical wave. If the scatterers were symmetrically arranged with interval d, these spherical waves would be synchronized only in the direction of the path length difference 2dsin equal to the integral multiple of wavelength and a part of the deflection angle 2 of the incident beam would generate a reflection point in the diffraction pattern. The X-ray with a known wavelength was used to measure the angle and to calculate the crystal plane spacing *d* for X-ray structural analysis, as shown in Fig. 3.

Fig. 3 – X-ray diffraction test instrument.

3. ANALYSIS OF EXPERIMENTAL RESULTS

3.1. Mechanical property analysis of composite materials

It can be seen from Table 3 that the compressive strength of the composites increased slowly within the first 7 days of curing, and then increased rapidly with the curing age. Adding expansive agent caused some expansion damage in the cement. When the amount of expansion agent was small, a small amount of ettringite, the hydration product, can effectively compensate for the pores and the self-shrinkage of the cement, and improve the early strength of the cement. When the content of the expansive agent was greater than 8 %, the early strength of cement developed slowly, but the later strength developed rapidly as the finished hydration, stable expansion, and the increase of cement stone matrix in the later hardening stage promoted rapid strength development. Excessive expansion agent makes the expansion deformation too large, the interior of the cement loose, and the surface prone to cracks [32]. The composite materials showed a certain early strength, which was conducive to the timely reinforcement of coal seams. With the curing age, the strength of the composites increased rapidly and reached the maximum after 28 days of curing.

Table 3

Uniaxial compressive strength results of composite materials

Test	Uniaxial compressive strength/MPa			
	3d	7d	14d	28d
A1	10.666	11.976	15.237	18.109
A2	8.479	12.044	13.392	15.495
A3	11.634	15.483	17.574	19.931
A4	11.927	12.796	16.139	20.848
A5	8.987	9.718	11.937	14.129
standard deviation	1.385	1.853	1.992	2.556

The stress-strain curve can reveal the deformation characteristics of the composite materials. The internal cracks occurred, expanded and break through during the uniaxial compression of the composite materials. The internal structure of the composite material became discontinuous from continuous. The stress-strain curves of the composite materials during 28 days of curing were compared in Fig. 4.

According to the stress-strain curves, the loading process of the materials can be divided into five stages: compaction stage, elastic stage, plastic stage, softening stage and residual strength stage. The specimens first entered the compaction stage, when the curve was concave upward, indicating that the pores in the material were gradually closed under the external force. With the increase of the load, the specimens entered the elastic stage when the pores in the material were compacted, and the stress-strain increased

linearly. The internal cracks gradually occurred, and the composites were still in a stable state. With further increase of the load, the composites entered the plastic stage when stress-strain increased nonlinearly, and an irreversible plastic change occurred, indicating that the internal cracks gradually expanded, penetrated and produced macroscopic cracks. When the peak load was reached, the composites entered the softening stage and expanded along the internal fracture surface. Macroscopic cracks increased deformation and decreased compressive strength. When the specimens were broken, the stress-strain of the material decreased rapidly to a relatively stable level as the friction between the internal fracture surfaces guaranteed a certain bearing capacity.

It can be seen that the stress-strain curves of the specimens are similar, but differ in the rising section. A5 serves as a blank control group. With the increase of expansive agent, water reducing agent and retarder content, the curve rose more gently, indicating the increase of the toughness of the composite. For specimens A1 and A3, where the cement accounts for a large proportion, the stress was mainly borne by the cement matrix, which was continuously compacted with the increase of load until the specimen was destroyed. Therefore, the specimens A1 and A3 entered the plastic stage earlier, and the deformation was relatively larger. With the decrease of water reducing agent and retarder, the cement particles were uniformly dispersed into the composite material, which enter the strengthening phase to improve the bearing capacity of the composite material. The uniaxial compressive strength of specimen A4 reached the maximum value of 20.848 MPa. When additives such as expansion agent were excessive, the uniaxial compressive strength of specimen A2 would decrease as the expansive agent and cement competed for water for hydration and inhibited each other. The hydration speed of the expansive agent was faster than that of the cement, generating a large number of expansion products AFt, resulting in expansion. The internal pores of the material are coarse, and the cement particles are not easy to be infiltrated by water for hydration reaction [33], and the cement matrix, the carrier of the composite material, transferred and loaded the stress. Low hydration degree of cement caused cracking under external force, and a large amount of accumulated elastic sharp release, making the cracks develop earlier. In other words, once the peak stress was reached, the composite would rupture immediately.

By analyzing the compressive strength and stress-strain of composite materials, it was found that additives such as expansion agents could significantly improve the mechanical properties of composite materials to a certain extent, but excessive expansion agents would bring defects, and decrease the strength. The composite material with 8 % expansive agent, 0.3 % water reducer and 0.03 % of retarder had low cost and high mechanical properties, and could adapt to drilling deformation, and was conducive to long-term coal seam reinforcement effect.

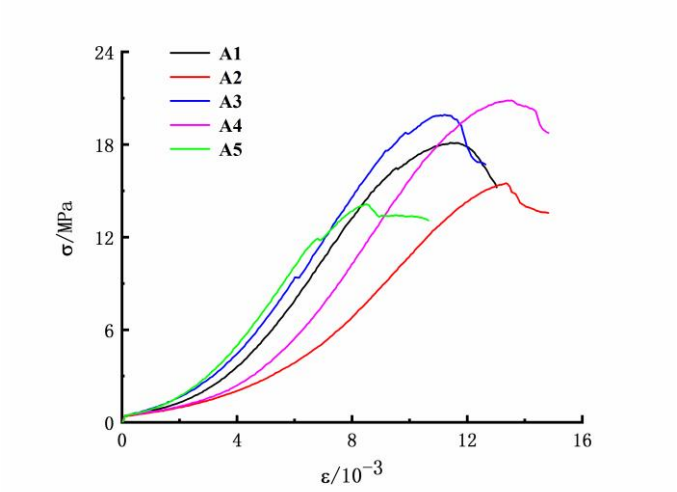

Fig. 4 – Stress-strain curves of composite material specimens.

3.2. Microstructure analysis of composite materials

Cut 2 ~ 3mm slice before SEM analysis, dry and spray gold at 27 KV. Analysis of voltage in vacuum environment. Figure 5a–5e is the result of electron microscope scanning of ultra-fine cement matrix

composite specimens cured for 28 days from A1 to A5. It can be seen that there were a large number of cement particles in the composite material, and the cement matrix skeleton and hydration products were intertwined into a dense network structure. During the loading process of the composite material, the cement matrix was first compressed to yield, and then the colloidal particles dislocation occurred, and the instability failure gradually occurred. Therefore, the plasticization ability of cement transferred stress and consumed energy in the composite material.

It can be seen from Fig. 5b that the interior of the cement of specimen A2, where the expansion agent content was large and the cement content was small was loose. When the external load increased, the expansive agent particles in the material were difficult to bear and disperse the stress, resulting in relatively low compressive strength. It can be seen from Fig. 5a and Fig. 5c that the hydration products were evenly embedded in the cement colloid, and the bonding points and contact area between the cement particles and the hydration products increased. The cement and the hydration product formed a stable continuous carrier with a more compact microstructure to bear the stress together, improving the compressive strength. A large number of expansion agent particles of specimen A4 are fully wrapped in the cement colloid, contributing to the tightest bonding at the interface between the cement and hydration products. and the improvement of the compressive strength. The internal pores of specimen A5 were relatively large, which seriously hindered the propagation of stress on the interface, resulting in poor mechanical properties.

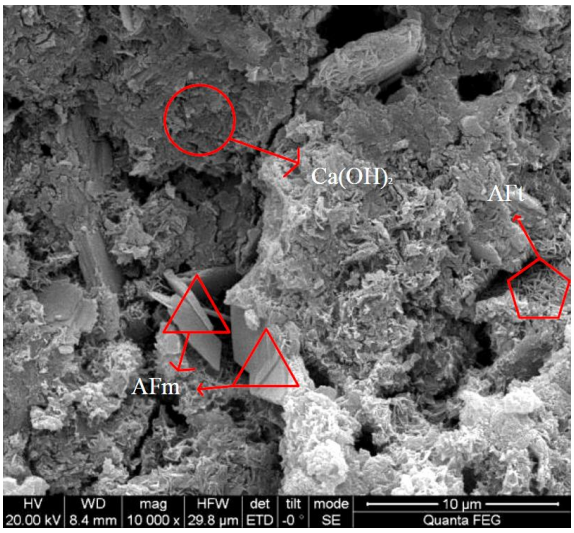

a) SEM of specimen A1

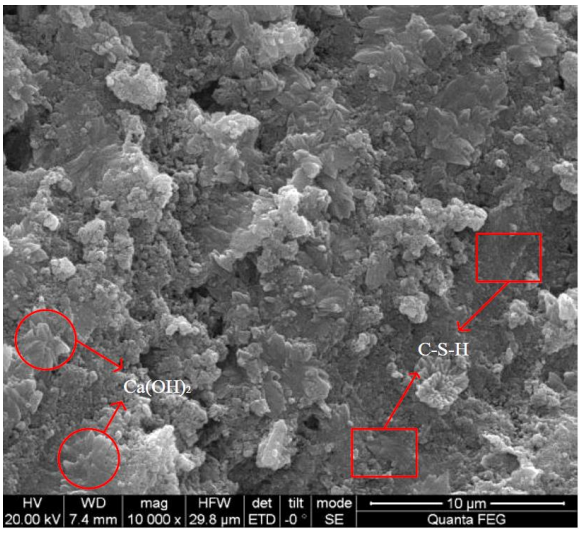

b) SEM of specimen A2

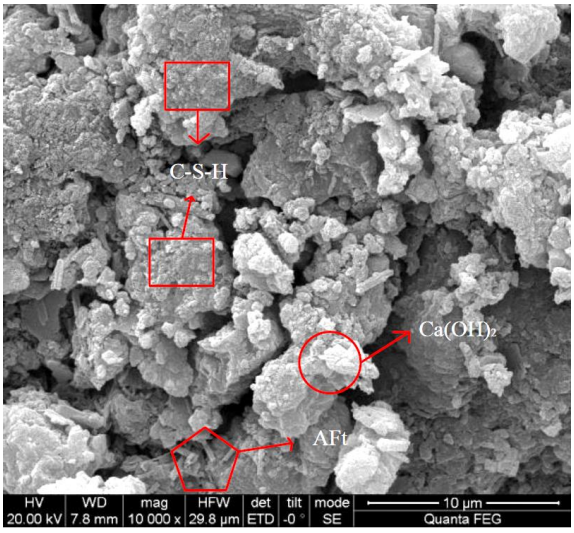

c) SEM of specimen A3

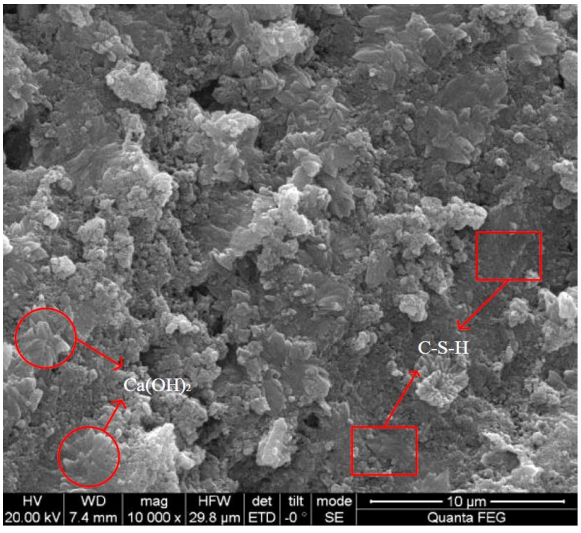

d) SEM of specimen A4

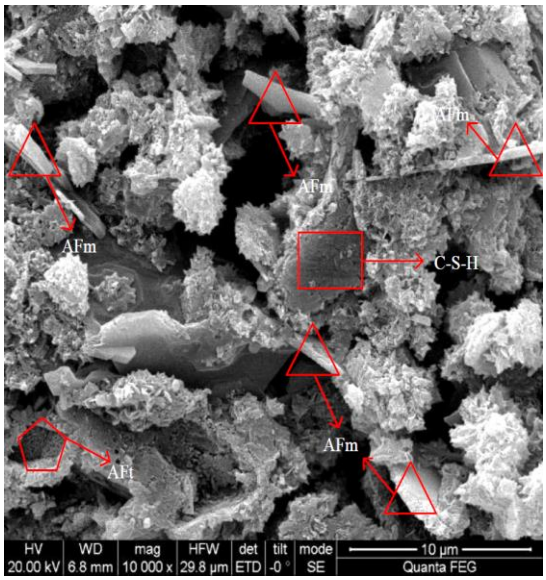

e) SEM of specimen A5

Fig. 5 – Microstructure morphologies of composite materials.

3.3. XRD analysis of composite materials

The results of XRD tests are shown in Fig. 6. It can be seen that the hydration products were significantly different after 28 days of curing. It can be seen from the XRD spectrum of specimen A5 that there were tricalcium silicate (C_3S), dicalcium silicate (C_2S), calcium hydroxide ($Ca(OH)_2$), ettringite in the system. The characteristic diffraction peaks of stone (AFt), calcium silicate hydrate (CSH), cement clinker minerals, especially C_3S and C_2S were relatively high, indicating that these minerals did not completely react. The diffraction peak intensity of $Ca(OH)_2$ was higher than that of AFt, resulting in low compressive strength of the material [34].

The characteristic diffraction peak intensity of Aft and C-S-H of the hydration products of specimen A4 increased continuously, and the hydration degree of the cement increased gradually. The intensity of $Ca(OH)_2$ diffraction peak was the weakest in the spectrum of specimen A4. Therefore, the compressive strength of specimen A4 was high. The rest of the spectra shown in Fig. 6 are the XRD spectra of specimens A1~A3. It can be seen that the diffraction peaks appearing in specimen A4 are exactly the same. The difference is that the AFt diffraction peak height is lower, while the $Ca(OH)_2$ diffraction peak intensity higher.

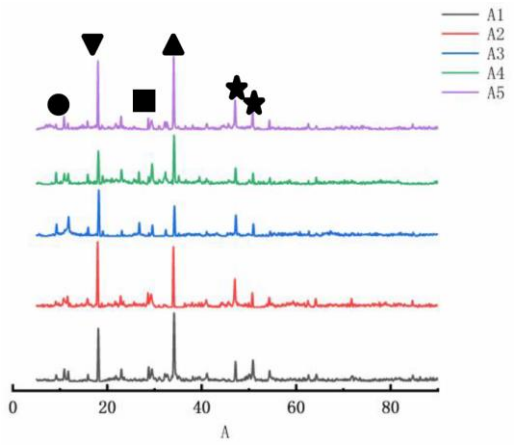

●—AFt; ▼—$Ca(OH)_2$; ■—C-S-H; ▲—$Ca(OH)_2$+C_3S+C_2S; ★—C_3S+C_2S

Fig. 6 – XRD pattern of composite materials under different ratio conditions.

4. CONCLUSION

1) A new sealing material with high mechanical properties was developed by using ultrafine cement as the basic material and adding additives, including water reducer, retarder, and expansion agent.

2) The amount of expansion agent significantly affects the mechanical properties of the composites. Less expansion agent is beneficial to improving the strength of the composites, and the excessive content will lead to defects, decreasing the mechanical strength. The composite with 8 % expansive agent, 0.3 % water reducer and 0.03 % retarder has high mechanical properties and obvious plastic characteristics.

3) The structure of pure cement, which is mainly affected by the type, quantity and form of cement hydration products, is relatively loose. The hydration is incomplete with a large number of C3S + C2S. The content of AFt in the hydration products is low. The ultrafine cement-based sealing material has a relatively dense structure and the hydration generates more AFt, contributing to a firm outer layer on the surface of cement particles, which improves the mechanical strength of the plugging material.

4) The SEM results show that the reason for the improvement of the mechanical properties of the material is that a large number of expansive agent particles are fully wrapped in the cement colloid, resulting in the most close bonding at the cement / hydration product interface. The bond strength of the two increases, which directly improves the compressive strength of the material. Thus affecting the improvement of strength.

ACKNOWLEDGEMENTS

All authors contributed to this paper. Xin Guo prepared and edited the manuscript. Xin Guo and Sheng Xue made a substantial contribution to the data analysis and revised the article. Xin Guo, Linfang Xie and Yaobin Li reviewed the manuscript and processed the Investigation during the research process. Sheng Xue and Chunshan Zheng provided fund support. We acknowledge the financial support for this work provided by the National Key Research and Development Program of China (2018YFC0808000), National Natural Science Foundation of China (51904013), Youth Science And Technology Talents Support Program (2020) by Anhui Association for Science and Technology (RCTJ202005), and Open Research Fund of State Key Laboratory of Coal Resources and Safe Mining, CUMT (SKLCRSM20KF003).

REFERENCES

1. L. YUAN, *Strategic thinking of simultaneous exploitation of coal and gas in deep mining*, Journal of China Coal Society, **41**, *1*, pp. 1-6, 2016.
2. A.T. ZHOU, K. WANG, *A new inorganic sealing material used for gas extraction borehole*, Inorganic Chemistry Communications, **102**, pp. 75-82, 2019.
3. Y.Y. CHENG, *Research on failure mechanisms of gas drainage through drilling in coal seam and efficient sealing technology*, Xuzhou, China University of Mining and Technology, 2014.
4. X.M. YUE, C.C XIAO, M. YE, Z.J. LIU, Z.Y. AN, S.Y. OUYANG, *Material fabrication and performance analysis of new gangue polymer*, Journal of Mining & Safety Engineering, **37**, *1*, pp. 169-175, 2020.
5. X.W. XIANG, C. ZHAI, Y.M. XU, X. YU, J.Z. XU, *A flexible gel sealing material and a novel active sealing method for coal-bed methane drainage boreholes*, Journal of Natural Gas Science and Engineering, **116**, *6*, pp. 1187-1199, 2015.
6. X.X. CHEN, R.Q. BI, L. ZHANG, *Effect of water-to-cement ratio on sulpho-aluminate type cementitious grouting materials*, Magazine of Concrete Research, **71**, *6*, pp. 298-308, 2019.
7. Q. WANG, L. WANG, B.H. LIU, B. JIANG, H.J. ZHANG, S. XU, *Study of void characteristics and mechanical properties of fractured surrounding rock grout*, Journal of China University of Mining and Technology, **48**, *6*, pp. 1197-1205, 2019.
8. Q. YUAN, D.J. ZHOU, H. HUANG, J.W. PENG, H. YAO, *Structural build-up, hydration and strength development of cement-based materials with accelerators*, Construction and Building Materials, **259**, p. 119775, 2020.
9. H.X. DING, S.Y. ZHANG, *Quicklime and calcium sulfoaluminate cement used as mineral accelerators to improve the properties of cemented paste backfill with a high volume of fly ash*, Materials, **13**, *18*, p. 4018, 2020.
10. J.P. ZHANG, L.M. LIU, Q.H. LI, W. PENG, F.T. ZHANG, J.Z. CAO, H. WANG, *Development of cement-based self-stress composite grouting material for reinforcing rock mass and engineering application*, Construction and Building Materials, **201**, pp. 314-327, 2019.
11. C. ZHAI, X.W. XIANG, Q.L. ZOU, X. YU, Y.M. XU, *Influence factors analysis of a flexible gel sealing material for coal-bed methane drainage boreholes*, Environ. Earth Sci., *5*, p. 385, 2016.

12. H.B. ZHANG, H.F. DI, Q.B. LIU, C.Y. HOU, D.D. ZHENG, H.C. CHAI, H.F. ZHOU, L. LIU, X.M. GUAN, *Research and application of micro-nano inorganic grouting materials*, Journal of China Coal Society, **45**, *3*, pp. 949-955, 2020.
13. X.M. GUAN, H.B. ZHANG, Z.P. YANG, H.Y. LI, J.J. LU, H.F. DI, B. SHUAI, C. XU, G.P. WANG, *Research of high performance inorganic-organic composite grouting materials*, Journal of China Coal Society, **45**, *3*, pp. 902-910, 2020.
14. S.C. Li, J. Zhang, Z.F. Li, Y.F. Gao, Y.H. Qi, H.Y. Li, Q.S Zhang, *Investigation and practical application of a new cementitious anti-washout grouting material*, Construction and Building Materials, **224**, pp. 66 – 77, 2019.
15. M. MOLLAMAHMUTOGLU, A. EYUBHAN, *Ultrafine Portland and cement grouting performance with or without additives*, Ksce Journal of Civil Engineering, **19**, *7*, pp. 2041-2050, 2015.
16. G. LUDWIK. GOLEWSKI, *Improvement of fracture toughness of green concrete as a result of addition of coal fly ash, characterization of fly ash microstructure*, Materials Characterization, **134**, pp. 335-346, 2017.
17. V.A. ARKHIPOV, D.Y. PALEEV, Y.F. PATRAKOV, A.S. USANINA, *Coal dust wettability estimation*, Journal of Mining Science, **50**, *3*, pp. 587-594, 2014.
18. H.K. HUSSAIN, G.W. LIU, Y.W. YONG, *Experimental study to investigate mechanical properties of new material polyurethane-cement composite(PUC)*, Construction and Building Materials, **50**, *2*, pp. 200-208, 2014.
19. J.X. ZHANG, Y.N. SUN, *Experimental and mechanism study of a polymer foaming grouting material for reinforcing broken coal mass*, KSCE Journal of Civil Engineering, **23**, *1*, pp. 346-355, 2019.
20. J.X. ZHANG, Y.N. SUN, Z.D. SUN, Z.M. WANG, Y.Y. ZHAO, T.B. SUN, *Analysis of macroscopic mechanical properties and Mechanism of coal dust/polymer composite grouting material*, Chinese Journal of Rock Mechanics and Engineering, **38**, *S1*, pp. 2889-2897, 2019.
21. H.T. WANG, X.C. WANG, M.H. ZHAI, S.C. LI, R.T. LIU, Z.F. LI, J.W. BAI, L.Z. ZHANG, J. AN, *Experiment and application of new material for grouting of gangue based aquifer*, Journal of China Coal Society, **42**, *11*, pp. 2981-2988, 2017.
22. Z.L. GE, X.D. MEI, Y.Y. LU, L. CHENG, B.W. XIA, J.F. CHEN, *Drilling sealed parameters and optimization of a new type sealing material for hydraulic fracturing in underground coalmines*, Journal of Basic Science and Engineering, **22**, *6*, pp. 1128-1139, 2014.
23. W.T. ZHANG, Y.S. ZHANG, Z.T. WU, N.D. LIU, D.F. YUAN, *Optimization design and properties of glass fiber reinforced cementitious composites*, Material Reports, **33**, *14*, pp. 2331-2336, 2019.
24. J.J. BAI, M. WANG, C.J. SHI, S.N. SHA, S.C. XIANG, B.B. ZHOU, Y.H. MA, *Design, synthesis of viscosity-reducing polycarboxylate superplasticizer and its influence on cement-silica fume paste with low water-binder ratio*, Material Reports, **34**, *3*, pp. 6172-6179, 2020.
25. Y. HE, X. ZHANG, M.D. GU, W.L. HONG, *Effect of organosilane-modified polycarboxylate-superplasticizer on fluidity and hydration process of cement paste*, Journal of the Chinese Ceramic Society, **44**, *8*, pp. 1166-1172, 2016.
26. X. GUO, S. XUE, C.S. ZHENG, Y.B. LI, *Experimental research on performance of new gas drainage borehole sealing material with high fluidity*, Advances in Materials Science and Engineering, 2021, p. 6645425.
27. K.L. ZHENG, X.H. YANG, R. CHEN, L.X. XU, *Application of a capillary crystalline material to enhance cement grout for sealing tunnel leakage*, Construction and Building Materials, **214**, pp. 497-505, 2019.
28. F. CHEN, B.L. HUANG, M.F. BA, X.D. BAO, *Experimental study on dual-fluid-grout composite materials with slag steel modified Portland cement and sodium silicate*, Acta Materiae Compositae Sinica, **30**, *6*, pp. 139-145, 2013.
29. H.Q. JIANG, Z.J. QI, E. YILMAZ, J. HAN, J.P. QIU, C.L. DONG, *Effectiveness of alkali-activated slag as alternative binder on workability and early age compressive strength of cemented paste backfills*, Construction and Building Materials, **218**, pp. 689-700, 2019.
30. D. HATUNGIMANA, C. TASKOPRU, M. ICHEDEF, M.S. MÜSLIM, Ş. YAZICI, *Compressive strength, water absorption, water sorptivity and surface radon exhalation rate of silica fume and fly ash based mortar*, Journal of Building Engineering, **23**, pp. 369-376, 2019.
31. Y. GUO, B.L. ZHANG, X.G. ZHENG, W. ZHOU, X.L. WEI, D.X. ZHU, *Grouting reinforcement technology of superfine cement with wind oxidation zone based on time-varying rheological parameters of slurries*, Journal of Mining & Safety Engineering, **36**, *2*, pp. 338-343, 2019.
32. B. LI, L.H. XU, Y.S. GU, L.L. JIA, *Investigation on the influence of HCSA expansive agent dosage on performance of high-strength self-compacting concrete*, Engineering Journal of Wuhan University, **50**, *1*, pp. 90-96, 2017.
33. J.J. FENG, M. MIAO, P.Y. YAN, *Hydration and expansion properties of shrinkage-compensating composite cementitious materials*, Journal of Building Materials, **15**, *4*, pp. 439-445, 2012.
34. N.S. MOHAMMAD, F.A. MOHAMMAD, J. SHIROKOFF, *Use of X-ray diffraction in assessing the aging pattern of asphalt fractions*, Fuel, **81**, *1*, pp. 51-58, 2002.

Received February 23, 2021